**Proceedings of the ASME 2010 International Design Engineering Technical Conferences &**
**Computers and Information in Engineering Conference**
**IDETC/CIE 2010**
**August 15-18, 2010, Montreal, Quebec, Canada**

# DETC2010-29186

# SAFETY OF SPUR GEAR DESIGN UNDER NON-IDEAL CONDITIONS WITH UNCERTAINTY

**Kyle Stoker**
Dept. of Mechanical & Aerospace Engineering,
University of Florida
Gainesville, FL 32611, U.S.A.

**Anirban Chaudhuri**
Dept. of Mechanical & Aerospace Engineering,
University of Florida
Gainesville, FL 32611, U.S.A.

**Nam Ho Kim**
Dept. of Mechanical & Aerospace Engineering,
University of Florida
Gainesville, FL 32611, U.S.A.

## ABSTRACT

The current practice of gear design is based on the Lewis bending and Hertzian contact models. The former provides the maximum stress on the gear base, while the latter calculates the contact pressure at the contact point between the gear and pinion. Both calculations are obtained at the reference configuration with ideal conditions; i.e., no tolerances and clearances. The first purpose of this paper is to compare these two analytical models with the numerical results, in particular, using finite element analysis. It turns out that the estimations from the two analytical equations are closely matched with those of the numerical analysis. The numerical analysis also yields the variation of contact pressures and bending stresses according to the change in the relative position between gear and pinion. It has been shown that both the maximum bending stress and contact pressure occur at non-reference configurations, which should be considered in the calculation of a safety factor. In reality, the pinion-gear assembly is under the tolerance of each part and clearance between the parts. The second purpose of this report is to estimate the effect of these uncertain parameters on the maximum bending stress and contact pressure. For the case of the selected gear-pinion assembly, it turns out that due to a 0.57% increase of clearance, the maximum bending stress is increased by 4.4%. Due to a 0.57% increase of clearance, the maximum contact pressure is increased by 17.9%.

**Keywords**: spur gear, gear design, contact, uncertainty analysis

## 1. INTRODUCTION

A gear is one of the most common mechanisms that transfer power from one machine to the other. From the design viewpoint, fatigue strength and wear are the most important criteria because each gear tooth may experience billions of load cycles. Thus, the gear design tends to incorporate a large safety margin and is usually over-conservative. For space applications, however, the weight of the system is an important constraint, and accordingly, much research has been carried out to reduce the system weight. For example, a deployable space structure such as the hoop-truss reflector in Harris corp., has more than a hundred gear-pinion pairs [1]. In such a case, a small weight reduction for each gear can reduce a significant amount of the total system weight. On the other hand, a small reduction in gear stress can cause significant change in expected fatigue life. For the case of mild steel, a 10% reduction in stress range can cause about a 50% change in fatigue life [2]. Thus, it is critically important to calculate stress accurately in gears. The objective of this paper is to evaluate the accuracy of the traditional, code-based gear design using computer-aided engineering tools and then evaluate the margin of safety under uncertainties that can happen during operating conditions. By providing for and designing gear trains that account for these uncertainties, a more accurate and predictable product can be produced.

The design of gear strength is based on two models: bending stress and contact stress models. The former is related to the stress at the gear base, while the latter is related to the wear at the contact surface. The bending equation was introduced by Wilfred Lewis in 1892. Since then, this equation has remained the standard for gear design [2, 3]. Lewis calculated stress in the gear base using a cantilevered beam under an applied bending moment. By using this simple model, an accurate bending stress could be determined [2]. This calculation assumes that the load is applied at the location of the pitch radius (i.e., reference configuration) [4]. In practice, however, contact between the gear and pinion occurs at various locations during the rotation.

Depending on the relative location between the gear and pinion, the magnitude and angle of the applied load may vary, affecting the bending stress at the base. This topic is extensively studied in this paper to illustrate the correlation that a numerical analysis can provide.

In addition to the bending equation, Heinrich Hertz was working on the spur gear problem around the year 1895. He developed an expression for the surface contact stress based on the maximum contact pressure between two cylinders [5]. He realized that the tooth profiles of the gear and pinion were similar to the convex shape of two cylinders in contact. By applying the necessary geometrical conditions of a spur gear to his model based on two cylinders in contact, a method for calculating the maximum contact stress of a spur gear was formulated [2]. In practice, however, the tooth profile is not a perfect cylinder, and the deflection of the tooth makes the contact condition non-Hertzian. A numerical analysis will be introduced for the comparison of the Hertzian contact stress to validate the results.

The current trend of gear design has begun to focus on innovative methods to design gears which are capable of handling higher loads [6]. Although the involute gear discussed in this paper is one of the most widely used gears in the industry, a number of other gear types exist which have recently come into use. A cycloidal gear profile offers a distinct advantage in terms of efficiency, but lacks the necessary load carrying capabilities [6]. Another design implements a gear profile based on a circular arc. These gears are capable of transmitting higher loads between gears but are very sensitive to manufacturing errors [6]. The deviation function has been introduced into the gear design industry to alleviate both the contact pressure and bending stresses in the gear teeth by modifying the surface profile [6]. This method analytically solves for the amount of sliding between contact points due to tooth profile modification. The amount of deviation from the pure rolling design can be incorporated into the function in order to design a new profile which reduces the amount of sliding.

In addition to the deviation function method for gear design, the optimization of existing designs has also been studied [7]. Several design variables which can be optimized to reduce both the contact pressure and bending stresses include the center distance, face width and pressure angle [7, 8]. By minimizing the amount of noise produced by gears in mesh, the authors were able to consider millions of designs that could potentially lead to a quieter, more efficient gear set [8]. Another optimization approach attempts to reduce the bending stress at the base of the gear tooth by optimizing the fillet radius in conjunction with finite element analysis [8]. By extending the limitations of the bending equation with the addition of FEA, along with fillet optimization, a reduction of bending stress on the order of 10-30% was realized [8].

The bending and contact stress models have typically been utilized at the reference configuration and ideal conditions of the spur gear model [9]. All tolerances in assembly and manufacture were assumed to be zero. This becomes a significant issue especially for space applications in which the gearbox is not stiff. In the application of these gears to real-world circumstances, this assumption cannot be valid. The common thread which unites all of these developing designs is the attempt to reduce the contact pressure and bending stress while maintaining a high level of efficiency. Thus, the pressure falls upon the manufacturer to produce gears that maintain a high level of accuracy in order to maintain the geometric constraints imposed by the designer. This paper studies the detrimental effects that manufacturing errors can have on both the contact pressure and bending stress. Certain manufacturing and assembly errors will always exist, which will unavoidably lead to errors in static and dynamic behavior [10]. In this paper, the contribution of assembly errors to static behavior of the gear model will be discussed. Specifically, the influence of the relative position between the gear and pinion and resulting effect on maximum bending stress and contact pressure will be analyzed.

## 2. ANALYTICAL METHODS OF GEAR DESIGN

### 2.1 Bending Stress at the Base

Lewis considered the tooth as a cantilevered beam and calculated the maximum stress at the root [2]. Although the ratio between the length and thickness is small, this approximation provides a reasonable estimate of the maximum stress, along with the stress concentration factor. Consider a cantilevered beam with length $L$, thickness $t$, and width $w$. When a contact force $F$ is applied at the tip, the maximum bending stress of the beam can be found as

$$\sigma_{\text{bending}} = \frac{6FL}{wt^2}. \tag{1}$$

The above formula is for a beam with a rectangular cross-section under an applied tip load. Although this serves as a good basis for gear design, the geometric effect of the gear and appropriate loading must be introduced. Consider a spur gear tooth in Figure 1. A horizontal force is applied at the location of the pitch radius. For the given loading condition, the maximum stress occurs at point $a$. By using similarity of two triangles in Figure 1, the following relation can be obtained:

$$x = \frac{t^2}{4L}. \tag{2}$$

Using Eq. (2), Eq. (1) can be rearranged as

$$\sigma_{\text{bending}} = \frac{3F}{2wx}. \tag{3}$$

The above equation can be further simplified by introducing a variable $y = 2x/3p$ with $p$ being the circular pitch. Then, the bending stress can be written as

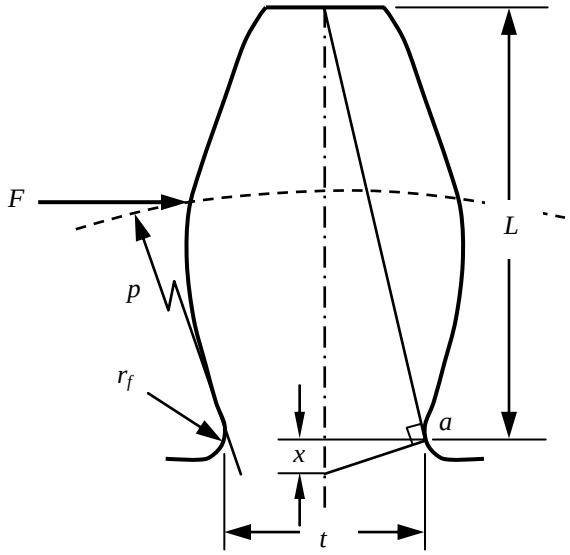


**Figure 1: Spur gear tooth geometry**

$$\sigma_{\text{bending}} = \frac{F}{wpy}. \tag{4}$$

Equation (4) has been the basis for the conventional gear design. In 1988, the American Gear Manufacturers Association (AGMA) has developed a formula for the bending stress which includes the effects of stress concentrations, such as fillet radius [11]. Since most gears experience millions of cycles, these stress concentrations will lead to a higher overall stress value, causing the fatigue life of the gear to decrease. The AGMA has provided the following equations to incorporate the stress concentration factor into the gear bending stress:

$$K_f = k_1 + \left(\frac{2y}{r_f}\right)^{k_2}\left(\frac{2y}{x_D - x}\right)^{k_3}. \tag{5}$$

Equation (5) solves for the fillet stress concentration factor by using the three constants $k_1$, $k_2$, and $k_3$, which were developed by Dolan and Broghamer [12]. In Eq. (5), $x$ and $y$ give the location of the maximum stress on the fillet radius. The determination of these values is an iterative process along with the gear bending equation to maximize the bending stress within the allowable range. In addition, $r_f$ is the fillet radius of curvature and $x_D$ is the point where the normal of the profile angle intersects the tooth center-line.

Once the stress concentration factor is calculated, the maximum bending stress is given as

$$\sigma_{\text{bending}} = \frac{w}{m}\cos\gamma_w \left[ K_f \left( \frac{1.5m\ \ x_D - x}{y^2} - \frac{0.5m\tan\gamma_w}{y} \right) \right]_{\max}, \tag{6}$$

where $m$ is the gear module, $w$ the load intensity, and $\gamma_w$ the angle between involute tangent and the tooth center-line at the load point. The maximum value of bending stress can be obtained by evaluating Eq. (6) along the entire length of the fillet radius. This approach is considered to be the most accurate because it accounts for the higher stresses that are invariable from the change in radius of the involute curve to the base of the gear [12]. This maximum value will be compared with the finite element analysis for validation purpose.

### 2.2Contact Stress

In addition to the bending stress at the base, the contact stress is an important design criterion. Hertz observed that two curved surfaces in contact can be modeled by two cylinders that are pressed together, creating a contact pressure [2]. The Hertzian contact stress was developed by utilizing the maximum pressure on the surface of two cylinders that are in contact. By a similar derivation as in the bending equation, the maximum contact pressure of two cylinders can be modified to introduce the geometry of the gear and pinion teeth in contact. When this geometry is introduced, the Hertzian contact stress is calculated as:

$$\sigma_C^2 = \frac{F}{\pi w\cos\phi}\frac{(1/r_1)+(1/r_2)}{\left[(1-\nu_1^2)/E_1\right]+\left[(1-\nu_2^2)/E_2\right]}, \tag{7}$$

where $\phi = \cos^{-1}(r_b / r)$ is the pressure angle, $r_b$ is the radius of base circle, $r$ is the pitch radius, $r_1 = \frac{1}{2}d_p\sin\phi$, $d_p$ is the pinion diameter, $r_2 = \frac{1}{2}d_g\sin\phi$, $d_g$ is the gear diameter, $\nu_1$ and $\nu_2$ are Poisson's ratios of pinion and gear, and $E_1$ and $E_2$ are the elastic moduli of pinion and gear.

Although the contact stress in Eq. (7) provides a reasonable estimate of contact stress on the gear, two different aspects of practical gear contact must be considered. First, the involute curve of the gear is not an exact cylinder, and the effect of neighboring non-cylindrical regions deviates the results from Hertzian contact conditions. In addition, when applied to a spur gear, the Hertzian contact stress assumes that the gear and pinion will be "perfectly" in contact. This means that the pitch radius point of the spur gear is in contact with that of the pinion. In practice, due to tolerances in manufacturing and clearance in assembly, the contact may not occur at the pitch radius location, which will be referred to as a non-ideal condition. Because of these assumptions, errors in the computation of safety factors can easily manifest themselves in assembly error [13].

## 3. NUMERICAL ANALYSIS USING NONLINEAR FINITE ELEMENT METHOD

The Lewis bending equation provides a reasonable estimate of the bending stress at the root of the gear tooth for many different gear dimensions and designs. Because of its simplicity and accuracy, the method remains popular to this day. However, with the advent of modern numerical analysis tools, the design

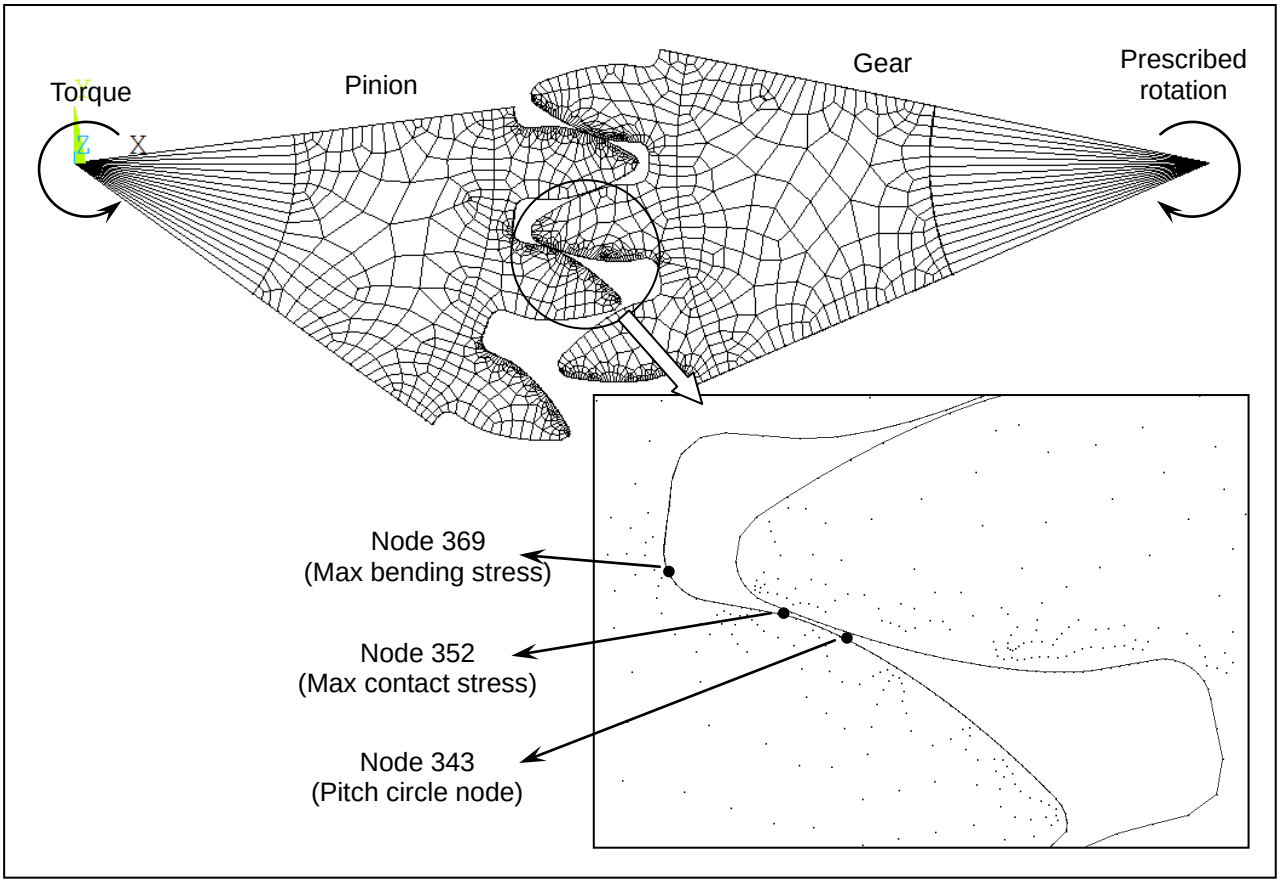


**Figure 2: Finite element model for spur gear assembly**

and evaluation of engineering concepts and devices can be explored more readily. In this paper, we use a finite element analysis program, ANSYS, to evaluate the accuracy of the two analytical models for gear design. The advantage of using finite element analysis software is that it can accurately consider the effect of detailed geometry, as well as complex loading conditions. Especially, it allows us to calculate the bending stress and contact pressure during the rotation of gears. In addition, it also allows us to calculate these two criteria under non-ideal conditions.

ANSYS Parametric Design Language (APDL) is used to create the gear and pinion model, apply contact and boundary conditions, control nonlinear solution sequence, and extract required analysis results. The code that was developed for this problem is separated into four different files, each of which serves its own purpose in defining parameters, creating the model, performing analysis, and extracting analysis results. The first file defines all variables that are required in constructing the gear geometries, material properties, finite elements mesh sizes, and applied loading conditions. Since all construction processes are parameterized, different gear assemblies can be constructed by modifying parameters in this file. Table 1 shows the required parameters and their values used in the numerical study.

**Table 1** *Input parameters for gear modeling and analysis*

| Pinion | | Gear | |
|---|---|---|---|
| No. of teeth | 25 | No. of teeth | 31 |
| Pitch dia. | 79.38mm | Pitch dia. | 98.43mm |
| Dia. of involute | 74.59mm | Dia. of involute | 92.49mm |
| Addendum | 4.43mm | Addendum | 4.18mm |
| Dedendum | 5.05mm | Dedendum | 5.30mm |
| Tooth thickness | 4.90 mm | Tooth thickness | 4.90mm |
| Face width | 31.75mm | Face width | 31.75mm |
| Root fillet radius | 1.04mm | Root fillet radius | 0.99mm |
| Tooth fillet radius | 0.78mm | Tooth fillet radius | 0.99mm |
| Elastic modulus | 206.8GPa | Elastic modulus | 206.8GPa |
| Poisson's ratio | 0.33 | Poisson's ratio | 0.33 |
| Center distance between pinion and gear | | 88.90mm | |
| Element size for teeth surface | | 0.1 | |
| Element size for body | | 1.0 | |
| Friction coefficient | | 0.0 | |
| Applied torque | | 800N-m | |

The second file consists of APDL commands that build a two-dimensional solid model including involute curves and generate finite elements (PLANE182 elements in ANSYS) using the automatic mesh generation functionality. Only three teeth are modeled because of periodic symmetry, which will significantly reduce the computational costs required to perform nonlinear finite element analysis of the model. This process is repeated for both the pinion and gear. Contact between the gear and pinion is established by defining contact elements on the edge of the gear teeth and target elements on the edge of the pinion teeth. Since contact pressures can only be calculated on the contact elements, the same procedure is repeated with contact elements on the pinion teeth and target elements on the gear teeth. Since initially the gear and pinion are not in contact, it can cause singularity if a torque is applied to the pinion. In order to prevent singularity, the pinion is rotated until it makes initial contact with the gear. The shaft portion is modeled using rigid elements that connect the gear inner surface to the node at the center of rotation. Both the gear and pinion are pinned at the center, but are allowed to rotate. Figure 2 illustrates the gear geometry that was created in ANSYS.

The third file is also an APDL program that controls nonlinear finite element analysis. It includes convergence criteria, automatic load stepping controls, and output request. The solution procedure consists of two steps. First, the torque at the center of the pinion is gradually increased until it reaches the full magnitude, while the center of gear is fixed to rotate. Next, the gear is rotated over a prescribed angle while the torque is held constant. The second step is divided by twenty increments so that smooth variation of stress and pressure can be obtained. Only the results from the second step are used for calculating bending stress and contact pressure. The fourth file performs postprocessing, which extracts deformed shapes, bending stresses, and contact pressures at each increment.

## 4. COMPARISON OF ANALYTICAL AND NUMERICAL RESULTS

In this section, the results from analytical methods (Section 2) and numerical methods (Section 3) are compared. In order to calculate analytical bending stress, it is necessary to calculate AGMA parameters in Eqs. (5) and (6) corresponding to the gear geometric parameters in Table 1, which are presented in Table 2. Then, the maximum bending stress calculated using the AGMA method and finite element analysis are compared in Table 3. It is important to note that in AGMA bending stress calculation, the location ($x$, $y$) that maximizes bending stress needs to be found by iteratively evaluating bending stress along the fillet radius. As most failures occur through tension in the gear [12], sampling points are chosen from the tension side of the fillet radius. Although the AGMA model and FEA calculation of the bending stress are close (0.7% difference), there is significant difference in the results. The AGMA model assumes that the applied torque is supported by a single tooth, whereas the FEA model shows that in most cases, either two or three teeth are in contact simultaneously, called a load sharing phenomenon. Especially when the bending stress is maximal, the load sharing ratio between two teeth is about 7:3. Thus, if the load sharing situation is considered, the AGMA model underestimates the bending stress by about 44%. Possible reasons for such a large difference are (1) the analytical model only considers bending stress, while the numerical model considers bending, shear, and axial stresses all together, (2) the contact force is not tangent to the pitch circle but perpendicular to the involute curve, and (3) the gear tooth is too short to be considered as a slender beam.

**Table 2** *Bending stress calculation parameters*

| Torque | 800 | N-m |
|---|---|---|
| $k_1$ | 0.18 | |
| $k_2$ | 0.15 | |
| $k_3$ | 0.45 | |
| $w$ | 827.81 | N/mm |
| $m$ | 2.59 | mm |
| $\gamma_W$ | 45.51 | degrees |
| $K_f$ | 1.18 | |
| $x_D$ | 43.44 | mm |
| $x$ | 34.45 | mm |
| $y$ | 3.71 | mm |

**Table 3** *Bending stress comparison*

| Method | Bending stress (MPa) | Difference |
|---|---|---|
| AGMA model | 578.7 | N.A. |
| FEA (2 teeth contact) | 582.8 | 0.7% |
| FEA (1 tooth contact) | 832.5 | 44% |

One of the advantages in finite element analysis is that the bending stress can be calculated at various rotational angles of the gear. Figure 3 shows the tensile and compressive bending stresses at the base of gear tooth as a function of rotational angles. It can be found that as the tooth rotates, the bending stress gradually increases and maintains almost a constant value for about ten degrees. At around eight degrees of rotation, the bending stress in both tension and compression drops significantly. This is due to three teeth being in contact simultaneously. Up until the point where the bending stress decreases, there are only two teeth in contact. For a few degrees of rotation, there are three teeth in contact, which reduces the bending stress by as much as 11%. Once the gear rotates further and only two teeth are in contact, the bending stress increases. This load sharing will be an important phenomenon when non-ideal conditions are introduced.

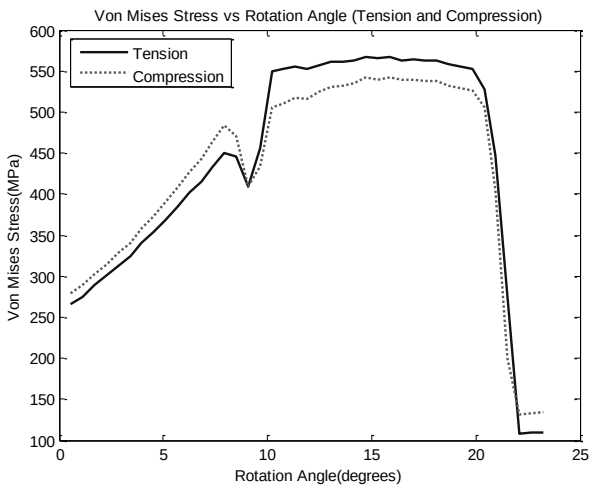


**Figure 3: Stress at gear tooth base (bending stress)**

For analytical calculation of contact pressure, Table 4 shows the Hertzian equation parameters corresponding to the gear geometric parameters in Table 1. Unlike the maximum bending stress, comparison in contact pressure is more complicated. First, the maximum bending stress occurs at a fixed location; the magnitude varies according to the rotation of the gear. However, the location of maximum contact pressure moves according to the rotation of the gear. In addition, it strongly depends on finite element discretization. Thus, it requires fine mesh along the contact surface (see Figure 2). Since the contact pressure is a local quantity, its value rapidly varies according to the rotation of the gear. Thus, instead of monitoring the maximum contact pressure at each rotation angle, the node that has the overall maximum contact pressure throughout the entire rotation of the gear is found first, and then, the variation of the contact pressure at that node is plotted as a function of the rotation of the gear. Because the finite element model is discrete and the contact pressure is calculated at nodes, non-zero contact stress values for a given node only occur for a few rotation angles. Figure 4 show this variation of contact pressure at the node that has overall maximum pressure (Node 341) and at the adjacent two nodes. These nodes are located near the tip of the tooth. Table 5 compares the contact pressure from Hertzian equation with that of finite element analysis. The difference of the contact pressure at the pitch radius location is about 4%. It is by accident that the Hertzian contact pressure at pitch circle location is close to the maximum contact pressure, which occurs at the different location. In terms of contact pressure at the pitch circle location, the difference is about 32%. The Hertzian model overestimates the contact pressure. Possible reason for such a large difference may be that the tooth profile is not cylindrical.

The most significant aspect of the contact pressure plot is the high magnitude of stress that can develop in the spur gear. These high levels of stress are only present for a small range of rotational angles. Over time, the oscillatory effect of these values can cause pitting and erosion due to fatigue stress [2]. Furthermore, if these values are increased over any portion of the gear or pinion, the amount of wear will increase. This increase in contact stress will be further investigated in the following section.

**Table 4** *Hertzian equation parameters*

| | | |
|---|---|---|
| $F$ | 26.28 | kN |
| $w$ | 31.75 | mm |
| $r_b$ | 30.44 | mm |
| $r$ | 79.38 | mm |
| $\Phi$ | 20.00 | |
| $d_p$ | 88.24 | mm |
| $d_g$ | 106.78 | mm |
| $R_1$ | 24.29 | mm |
| $R_2$ | 32.76 | mm |
| $\nu_1 = \nu_2$ | 0.33 | |
| $E_1 = E_2$ | 206.8 | GPa |

**Table 5** *Contact stress comparison*

| Method | Location | Contact stress | Difference |
|---|---|---|---|
| Hertzian model | Pitch circle | 1511 | N.A. |
| FEA (Node 341) | Tooth tip | 1574 | 4% |
| FEA (Node 351) | Pitch circle | 1029 | 32% |

## 5. NON-IDEAL LOADING CONDITIONS

With any mechanical assembly, there are tolerances and clearances which are applied to each part of the assembly. As the different parts are assembled, these tolerances can interact to affect how the total tolerances of the entire assembly are maintained. In addition, the flexibility of the gearbox can cause misalignment of axes. These can cause gaps, misalignments, slips, twists, etc, which are referred to as non-ideal conditions in this paper. For a spur gear and pinion idealized into a two dimensional system, there are a limited amount of non-ideal conditions which can be considered. The type of non-ideal condition that will be discussed is the amount of axial separation between the gear and pinion. Due to the tolerances in the shafts of the gear and pinion, the axial separation between the two can vary by as much as $0.02$" if the tolerance on the gear and pinion shafts is within $\pm 0.01$" [14]. The effect that this separation on the bending stress and contact pressure will be evaluated.

As the distance between the gear and pinion is increased, the bending stress and contact pressure will increase due to the elongated moment arm. At nominal or ideal conditions, the separation between the gear and pinion should be $88.9\text{mm}$. Due to the tolerance stack up, the amount of separation can vary as much as $0.02$" or $0.508\text{mm}$. The effect of axial separation on the bending stress is illustrated in Figure 5. The axial separation is first increased by $0.01$" and then by $0.02$". The effect of load

 

sharing by three teeth almost disappears at a clearance of $0.01$". When the clearance is $0.02$", the bending stress has increased in both tension and compression over the majority of the plot. The maximum stress increases about $5\%$ over the nominal configuration (see Table 6 for numerical values). An important aspect of this plot is how the increase in the axial separation changes the load sharing capability of the gear and pinion. Instead of the bending stress decreasing due to three teeth being in contact, the bending stress increases. The increase in axial separation eliminates the three teeth in contact, and the bending stress rises due to the higher load on the pinion tooth. Once contact on the third pinion tooth is encountered, the bending stress finally begins to decrease. The difference in values at this critical point can be as much as a $42\%$ increase in the bending stress. In addition, the maximum value of bending stress occurs at different locations. In ideal conditions, the maximum occurs at fifteen degrees of rotation, which corresponds to contact at the pitch radius location. On the other hand, in the case of $0.02$" separation, the maximum stress occurs at eight degrees of rotation, which corresponds to the lack of load sharing point. This data implies that as normal tolerances and assembly practices are utilized, the tolerance stack up can very easily lead to the type of situation shown above. This effect will be amplified when the gearbox is not stiff enough such that its deformation is not ignorable. This increase in the bending stress will cause more wear and fatigue on the root of the gear. Over time, an increase in these parameters will cause the gear to fail before its intended lifetime.

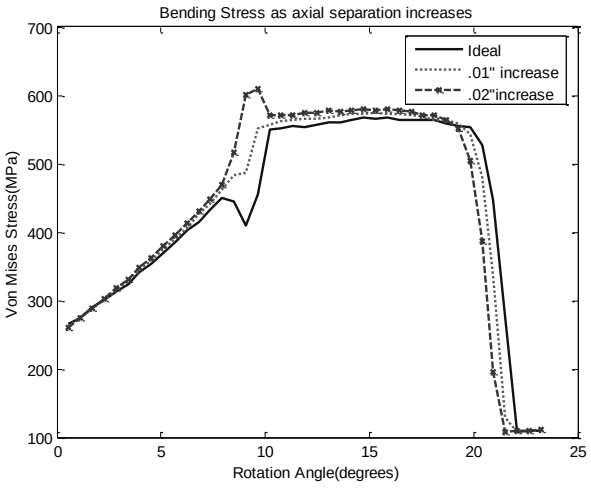


**Figure 4: Variation of bending stress with increasing axial separation**

**Table 6** *Increase in bending stress as axial separation increases*

| Nominal distance | Non-ideal distance ($0.02$" increase) | Percent difference |
|---|---|---|
| 582.8 MPa | 611.5 MPa | 5.0% |

**Table 7** *Non-ideal loading conditions on contact stress*

| Nominal distance | Non-ideal distance | Percent difference |
|---|---|---|
| 1029 MPa | 1213 MPa | 17.9% |

Next, a similar approach is taken for the contact stress between the gear and pinion. For this contact stress analysis, three nodes were chosen along the contact profile of the gear and pinion; their locations corresponded to the pitch circle of the pinion. This is necessary because the contact point moves along with the rotation of the gear as well as the axial separation. Figure 6 plots the variations of contact pressures for these three nodes at the nominal and non-ideal conditions. The first portion of this plot contains the baseline values for the nominal clearance. Next, the axial separation was increased by $0.02$", and resulting contact pressures were plotted. For each of the three nodes, the contact stress increased. The maximum increase occurred at the first node and was found to be $17.9\%$ greater, as shown in Table 7.

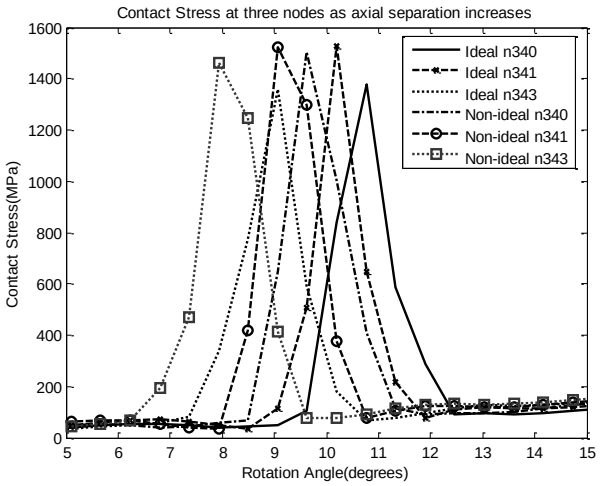


**Figure 5: Variation of Contact stress with increasing axial separation**

Due to this increase, engineers must take into account the effect that the axial separation has on the contact stress. It has been shown that the amount of wear is directly proportional to the contact pressure [15]. If certain areas of the gear and pinion experience higher contact stress levels, the wear will increase. Over billions of cycles, the increase in contact stress will become significant enough to increase the wear past what is predicted to be within the safety factors. This wear will ultimately cause the destruction of the gear train.

## 6. UNCERTAINTY ANALYSIS USING SURROGATE MODELS

Thus far, the spur gear analysis has assumed that the only parameter which varies is the axial separation between gear and pinion. By increasing or decreasing this separation the response

of the gear, bending and contact stresses will change. In practice, there are many other parameters that could also affect the stresses, including Young's modulus, applied torque, accuracy of tooth shape, etc. In order to predict bending and contact stress more accurately, the effect of these parameters need to be considered. However, these parameters are, by nature, uncertain due to variability of material properties, tolerances in manufacturing, and the random nature of applied torques. In such a case, it is more appropriate to perform uncertainty analysis and evaluate the reliability of gear assembly in terms of probability of failure, rather than the maximum values of stresses. In this section, uncertainty analysis will be performed for the bending and contact stress.

### 6.1. Input Uncertainty Quantification

In order to calculate the uncertainty of stresses, it is first necessary to estimate the uncertainties in input parameters. Among many parameters that can affect the uncertainty of stresses, three parameters that can affect the stress the most are chosen: Young's modulus, axial separation, and applied torque. If probability distributions of these parameters are known, they can be used in uncertainty analysis. However, since accurate distributions are not available, they are assumed to be uniformly distributed within the ranges of typical engineering applications. The purpose is to demonstrate the effect of uncertain input parameters on the bending and contact stresses.

The uncertainty in Young's modulus comes from variability in the manufacturing process. Although different processes may have different ranges of variability, it would be reasonable to choose the range to be $\pm 10\%$ of its nominal value. For this analysis, Young's modulus may range from $186.12$ to $227.48\mathrm{GPa}$. The applied torque depends on the power from motors and the gear ratio, and accordingly, its range is widely distributed. However, design of gears focuses on the maximum level of torques, which has a much smaller variation. The major sources of variability are transmission errors and wear of the gear teeth, which is assumed to be uniformly distributed in the rage of $\pm 5\%$ of its maximum value. The torque may, therefore, range between $760$ to $840\mathrm{N{\cdot}m}$. Finally, the range of the axial separation is the same as for non-ideal loading conditions, from $88.9$ to $89.408\mathrm{mm}$, based on tolerances.

### 6.2. Surrogate-Based Uncertainty Propagation

The uncertainties in input parameters propagate through governing equations (in this case, finite element analysis) and produce uncertainty in outputs (i.e., bending and contact stresses), which is called uncertainty propagation. There are many different methods for uncertainty propagation, including the Monte Carlo simulation (MCS, [16]), the first-order reliability method (FORM, [16]), the second-order reliability method (SORM, [16]), the stochastic response surface method (SRSM, [17]), the dimension reduction method (DRM, [18]), etc. Except for MCS, all other methods approximate output using a simplified form in order to reduce computational costs. In addition, some methods are accustomed to calculating the level of reliability but do not provide the entire probability distribution of the output. Thus, in this paper, MCS is utilized to evaluate the uncertainty distribution of bending and contact stresses. The challenge in MCS is computational costs because it requires numerous numbers of samples, and each sample requires solving nonlinear finite element analysis. In order to overcome the computational cost issue, a surrogate modeling technique [18] is used, which approximates the output as an explicit function of input parameters. Once this functional form is available, MCS can be performed on the surrogate model with numerous numbers of samples. An important issue in surrogate modeling is the accuracy of the model. The strategy that has been chosen in this paper is to build multiple surrogates and to select the best one in terms of various error measures.

The first step in surrogate modeling is the design of experiments. In this step, a number of samples of input parameters are selected, and finite element analyses are performed with these values of input parameters to evaluate the values of output. Then, the parameters of the surrogate model are calculated using the combinations of inputs and outputs by minimizing errors between outputs and predicted values from the surrogate model. Since two outputs (bending and contact stresses) are considered, two separate surrogate models need to be generated. As more sampling points are used, the surrogate model becomes more accurate. Since there are three input parameters, a total of twenty-eight samples are generated using the Latin Hypercube sampling method [18], which means that the same number of finite element analyses are performed.

In this paper, the Surrogate Toolbox for MATLAB program [19] is used to generate five different surrogate models: Kriging (KRG), polynomial response surface of order 1 (PRS1), PRS of order 2 (PRS2), radial basis neural network (RBNN), and support vector regression (SVR). The same sampling data from the Latin Hypercube sampling are provided to all surrogate models. Table 8 shows the most common four error measures that are used to evaluate the accuracy of the five surrogate models for the maximum bending stress. Even if KRG is the best for $\mathrm{R}^2$ values, this is due to the interpolating property of KRG. Among different error measures, $\mathrm{PRESS}_{\mathrm{RMS}}$ is the most reliable measure to estimate the error at non-sampling points. Thus, based on $\mathrm{PRESS}_{\mathrm{RMS}}$, it can be concluded that PRS1 and PRS2 are better fits than the rest of other three surrogate models. Since the $\mathrm{R}^2$ and $\mathrm{R}^2_{\mathrm{adj}}$ values for these two surrogate models are close, it is difficult to select one over the other. In such a case, it would be better to select one based on t-statistics of coefficients. It is generally suggested that the t-statistics of coefficient must be greater than $-2$, in order to have robust values of coefficients. Table 9 shows t-statistics for the coefficients of PRS1 and PRS2. It is clear that the coefficients of PRS1 are much greater than $-2$ and thus, more stable. Thus, PRS1 is selected to be the best surrogate model for the maximum bending stress.

Similar procedures are repeated for the contact stress. Based on error measures in Table 10, PRS1 and PRS2 are again chosen as the best candidates according to $PRESS_{RMS}$. Since the $R^2$ and $R^2_{adj}$ values for PRS1 and PRS2 models are similar, the t-statistics of these two surrogate models are compared in Table 11. Since the t-statistics values of most coefficients for PRS1 are lesser than $-2$, PRS2 is selected to be the best surrogate model for the maximum contact stress.

**Table 8** *Errors for the different surrogate models for bending stress*

| Surrogate Models | $PRESS_{RMS}$ | $RMS_{PRED}$ | $R^2$ | $R^2_{adj}$ |
|---|---|---|---|---|
| PRS1 | 10.77 | 10.23 | 0.83 | 0.81 |
| PRS2 | 11.95 | 10.41 | 0.87 | 0.80 |
| KRG | 17.49 | Infinite | 1.0 | NaN |
| RBNN | 18.29 | Infinite | 0.95 | 0.95 |
| SVR | 62.58 | Infinite | 1.0 | 1.0 |

**Table 9** *t-statistics of the coefficients of PRS1 and PRS2 for bending stress*

| Surrogate Model | t-statistics of the coefficients |
|---|---|
| PRS1 | [85.68; 5.14; 0.14; 8.90] |
| PRS2 | [27.87; 1.74; 1.82; 2.52; -0.18; -1.64; -0.02; -1.42; -0.02; -0.92] |

**Table 10** *Errors for the different surrogate models for Contact Stress*

| Surrogate Models | $PRESS_{RMS}$ | $RMS_{PRED}$ | $R^2$ | $R^2_{adj}$ |
|---|---|---|---|---|
| PRS1 | 45.80 | 42.33 | 0.65 | 0.61 |
| PRS2 | 57.10 | 44.99 | 0.70 | 0.56 |
| KRG | 63.24 | Infinite | 1.0 | NaN |
| RBNN | 106.47 | Infinite | 0.97 | 0.97 |
| SVR | 165.92 | Infinite | 1.0 | 1.0 |

**Table 11** *T-statistics of the coefficients of PRS1 and PRS 2 for contact stress*

| Surrogate Model | t-statistics of the coefficients |
|---|---|
| PRS1 | [63.70; -3.89; -5.19; -2.23] |
| PRS2 | [20.89; -1.16; 0.03; -0.97; 0.55; 0.07; 0.23; -1.05; -0.13; 0.53] |

**Table 12** *Mean and standard deviation of maximum bending and contact stresses*

| Type of Stress | Mean (MPa) | Standard Deviation |
|---|---|---|
| Max Bending Stress | 571.80 | 18.82 |
| Max Contact Stress | 1465.63 | 54.62 |

## 6.3. Uncertainty Analysis Using Surrogate Models

The last step of the uncertainty analysis involves generating a large number of sample points for MCS in order to estimate the statistical property of bending and contact stresses. Within the lower and upper bounds of the three input parameters, 100,000 random samples are generated using their probabilistic distribution types. Then, 100,000 numbers of bending and contact stresses are calculated from their surrogate models, from which the statistical distribution of them can be estimated. The results of these data will give expected stress values to within a certain degree of accuracy. These values can be compared to typical safety factor estimations and the number of failed designs can be determined if the failure stress information is available.

The results for the MCS for maximum bending and contact stress are shown in the form of histograms in Figures 7 and 8. The mean values and the standard deviations of the simulation are listed in Table 12 for each case. It can be seen that the mean values for both the cases are close to the numerical analysis values computed using ANSYS at the mean values of the three parameters. It is noted that the distributions in Figures 7 and 8 are obtained based on the given distributions of input parameters.

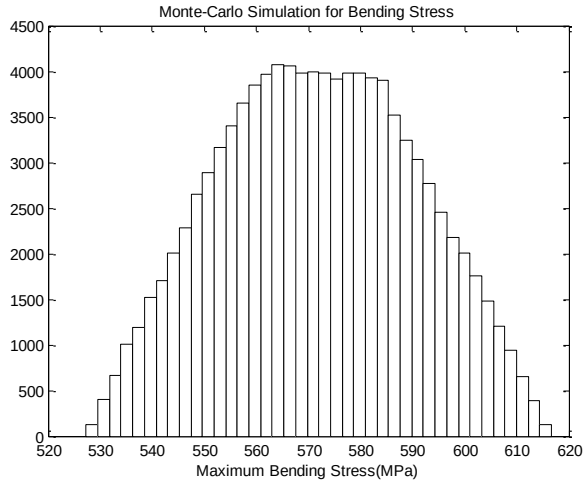


**Figure 6: Histogram showing the distribution of maximum bending stresses for 100,000 data points as estimated by the surrogate model PRS1**

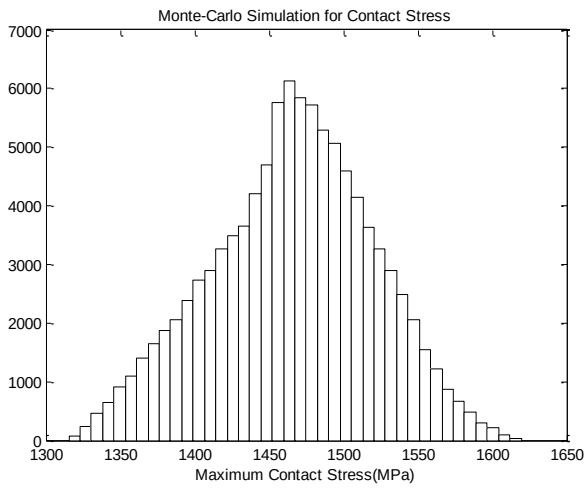


**Figure 7: Histogram showing the distribution of maximum contact stresses for 100,000 data points as estimated by the surrogate model PRS2**

## 7. CONCLUSIONS

A method to properly develop the gear and pinion geometries has been developed parametrically in ANSYS. With the help of this program, the implementation of many different geometrical configurations can easily be obtained. The finite element method is a good means to solve this problem for a spur gear model.

By implementing the necessary parameters into the gear code, it is possible to simulate real world gears. The AGMA bending equation and the Hertzian contact equations are the basis for which engineers design gears to this day. By comparing the analytical results obtained from these equations to the numerical analysis results under the same exact configurations, the accuracy of the numerical analysis can be verified. The correlation between the values was shown to be within .46% for the bending stress and 4% for the contact stress. These values correspond very well to the analytical solutions which confirm the validity of the program.

Once the validity of the program was verified, the effects of the non-ideal loading conditions were taken into account. Because engineers specify the tolerances to within what the assembly deems acceptable, the range of these values should be investigated. As the axial separation was increased, both the bending stress and the contact pressures increased. With a 0.57% increase in the axial separation between the gear and pinion, the bending stress increased by 4.4%. Also, with a 0.57% increase in the axial separation between the gear and pinion, the contact stress increased by 17.9%. The increase in axial separation also caused the positive effects of load sharing to be decreased. The load sharing capability was reduced from three teeth to two, and a difference of 49% in the predicted bending stress was shown. This increase in bending stress is substantial and would greatly reduce the factor of safety due to the decrease of fatigue life.

From the conclusions drawn through this paper, a number of important points were developed. When an engineer uses the Hertzian contact stress equation to solve for the maximum values that he or she expects the gear to be subjected to, one must realize that the configuration of the gear plays an important role. As the gear and pinion rotate through their contact areas, the contact stress can increase by large amounts. Although these values may only exist for a short period of time, their effects on the wear of the tooth can be pronounced. This increased wear can account for the failure of a gear before its predicted life cycle. To properly engineer around this problem, the solution can take one of two forms. The type of material and hardening techniques can be improved so as to obtain a better resistance to wear. However, an increased production cost of the gear may come with this type of solution. Another solution would be to increase the size and thicknesses of the gears being used. This would lead to more material and a heavier final product.

In addition to the increase in contact stress, the effects of non-ideal loading conditions cannot be ignored. The tolerance stack up will yield end products that have discrepancies in their axial separation on the same level that was presented in this paper. A tool which can accurately and quickly determine how these non-ideal conditions affect the wear of the tooth will be a very useful commodity. By understanding the processes that occur under these conditions, a better and more thorough design of the spur gear can be obtained.

## ACKNOWLEDGEMENT

This work was supported by the National Research Foundation of Korea (NRF) grant funded by the Korea government (MEST) (No. 2009-0081438, No. 2008-02-010), Deere and Company, and National Science Foundation (CMMI-0600375).

## REFERENCES

[1] Deployable Antennas, Harris Corp., Website: http://www.harris.com/igs/video/ IGS_2008/02_DeployableAntenna.pdf

[2] Shigley, Joseph Edward. Mechanical Engineering Design / Joseph E. Shigley, Charles R. Mischke, Richard G. Budynas. – 7th ed.

[3] Dudley, Darle W. Handbook of practical gear design, Mcgraw-Hill, 1984

[4] Colbourne, J.R., The Geometry of Involute Gears, Springer-Verlag, 1987

[5] Hertz, Heinrich. Ueber die Beruehrung elastischer Koerper (On Contact Between Elastic Bodies)," in Gesammelte Werke (Collected Works), Vol. 1, Leipzig, Germany, 1895.

[6] Yeh, Thomas, Yang, Daniel C.H., Tong, Shih-Hsi, Design of New Tooth Profiles for High-Load Capacity Gears, Mechanism and Machine Theory, Volume 36, Issue 10, October 2001, Pages 1105-1120

 

[7] Harianto, Johnny, Houser, Donald R., A Multi-Variable Approach to Determining the "Best" Gear Design, 2000 ASME Power Transmission and Gearing Conference, September 10-13, Baltimore, Maryland, USA
[8] Kapelevich, Alexander L., Shekhtman, Yuriy V., Direct Gear Design: Bending Stress Minimization, Gear Technology, 2003
[9] Anderson, Flodin , Andersson, Sören. Simulation of mild wear in helical gears Wear Volume 241, Issue 2, 31 July 2000, Pages 123-128
[10] H. Ding, & A. Kahraman, Interactions between nonlinear spur gear dynamics and surface wear, Journal of Sound and Vibration (2007), doi:10.1016/j.jsv.2007.06.030
[11] AGMA Standard, Fundamental rating factors and calculation methods for involute spur and helical gear teeth, ANSI/AGMA 2001-B88, Alexandria, VA, 1988
[12] T. J. Dolan and E. L. Broghamer, A photoelastic study of stresses in gear tooth fillet, University of Illinois Engineering Experiment Station, Bulletin No. 335, 1942
[13] Barber, J.R., Ciavarella, M. Contact Mechanics International Journal of Solids and Structures Volume 37, Issues 1-2, January 2000, Pages 29-43
[14] Earle, James H. Graphics Technology , Pearson Prentice Hall
[15] Kim, Nam Ho, Won, Dongki, Burris, David, Holtkamp, Brian, Gessel, Gregory R., Swanson, Paul, Sawyer, Gregory W, Finite element analysis and experiments of metal/metal wear in oscillatory contacts